Ionisable emerging pharmaceutical adsorption onto microwave functionalised biochar derived from novel lignocellulosic waste biomass

Paunovic, Olivera; Pap, Sabolc; Maletic, Snezana; Taggart, Mark A.; Boskovic, Nikola; Turk Sekulic, Maja

Published in:
Journal of Colloid and Interface Science

Publication date:
2019

Ionisable emerging pharmaceutical adsorption onto microwave functionalised biochar derived from novel lignocellulosic waste biomass

Olivera Paunovic[a], Sabolc Pap[a,b,1], Snezana Maletic[c], Mark A. Taggart[b], Nikola Boskovic[a], Maja Turk Sekulic[a,2]

[a] *University of Novi Sad, Faculty of Technical Sciences, Department of Environmental Engineering and Occupational Safety and Health, Trg Dositeja Obradovica 6, Novi Sad, Serbia*

[b] *Environmental Research Institute, North Highland College, University of the Highlands and Islands, Thurso, Scotland, KW14 7JD, UK*

[c] *University of Novi Sad, Faculty of Science, Department of Chemistry, Biochemistry and Environmental Protection, Trg Dositeja Obradovića 3, Novi Sad, Serbia*

[1]Corresponding author at: Environmental Research Institute, North Highland College, University of the Highlands and Islands, Thurso, Scotland, KW14 7JD, UK

[2]Corresponding author at: Department of Environmental Engineering and Occupational Safety and Health, Faculty of Technical Sciences, University of Novi Sad, Trg Dositeja Obradovica 6, Novi Sad, Serbia

E-mail addresses: sabolcpap@uns.ac.rs; szabolcs.pap@uhi.ac.uk (Sabolc Pap); majaturk@uns.ac.rs (Maja Turk Sekulic)

Graphical abstract

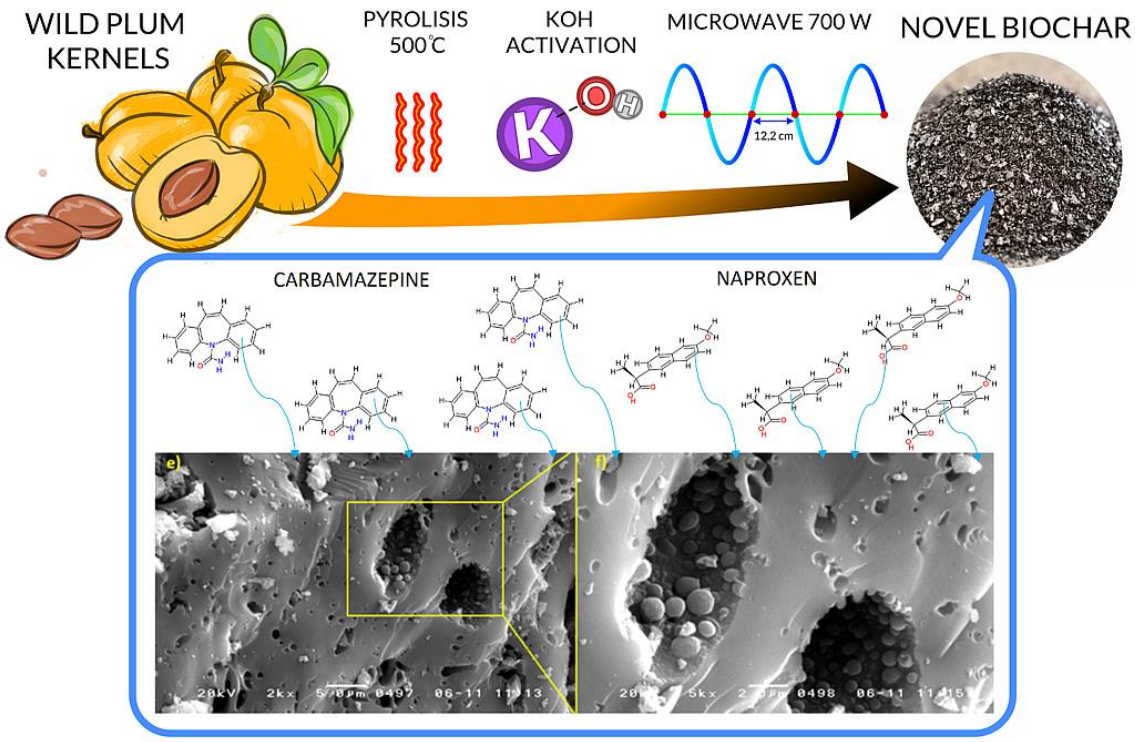

Abstract

Functionalised biochar (WpOH) was prepared from wild plum kernels using simultaneous pyrolysis and microwave potassium hydroxide (KOH) functionalisation. This was then applied to the removal (from water) of an ionisable pharmaceutical - naproxen (NPX). Characterization of the WpOH was carried out using pH_{pzc}, SEM/EDX, BET, FTIR, XRD, and the principle adsorption mechanisms were thoroughly studied. A pseudo-second order kinetic model best described the reaction kinetic behaviour, and the Langmuir isotherm provided the best fit to the results. The maximum adsorptive interaction (73.14 mg/g) occurred between pH 5 and 7 through electrostatic attraction (the main interaction mechanism) between the negatively charged NPX and the positively charged WpOH functional groups. In addition, hydrogen-bonding and electron-donor-acceptor (EDA) interactions were important. In a

competitive study, using NPX and carbamazepine (a basic/amphoteric drug), the different nature/structure of the two compounds resulted in slight competitive adsorption. The results demonstrate the potential for wild plum kernel biochar to be used in the efficient removal of emerging contaminants such as pharmaceuticals from water.

Keywords: Microwave functionalised biochar; Emerging pharmaceutical compounds; Adsorption; Mechanisms; Competitive adsorption

1. Introduction

Water pollution and security remain critical Global Challenges and sustainable solutions are needed to protect water resources and remove pollutants. Among the many pollutants found in water, emerging contaminants (such as, pharmaceuticals, flame retardants, endocrine disrupting compounds, disinfection by-products, etc.) are a priority as they may cause a risk to wildlife and human health, and their environmental impacts are not yet fully understood. Potential negative effects of emerging contaminants (ECs) in the environment depend on factors such as lipophilicity, biodegradability, bioaccumulation potential, concentration and exposure time. Over the last fifteen to twenty years, bioactive pharmaceuticals (PhCs) have been receiving increasing attention as pollutants in aquatic environments. They are considered emerging pollutants as they largely remain unregulated, or, are currently going through regulatory assessment [1]. Once PhCs reach the environment, unintended effects may occur in wildlife (i.e., in non-target organisms), eliciting physiological change, which may then lead to negative population level effects [2]. Naproxen (NPX; (+)-2-(6-metoxy-2-naphtyl) propionic acid) is a non-steroidal anti-inflammatory drug (NSAID) (Table S1). It possesses analgesic, antipyretic, and anti-inflammatory effects [3]. NPX

(as a contaminant) has been detected all over the world, at up to 2.3 µg/L in wastewater effluent, highlighting the fact that this (and many other PhCs) are often not effectively removed by conventional wastewater treatment [4]. NPX is also now on the Global Water Research Coalition (GWRC) priority list, and is a more common NSAID than diclofenac in Scotland (following significant increases in recent dispensing rates). Carbamazepine (CBZ) – also considered herein - is an antiepileptic drug and one of the most frequently detected PhCs in wastewater [5]. Treated effluents have been noted to contain high levels (up to 2.1 µg/L) (Table S1) [6].

Water treatments that can be used to remove PhCs from wastewater include: adsorption [7], advanced oxidation [8], ultrasonic treatment [9], carbon nanotube membranes [10], biological processes [11] and photocatalysis [12], as well as various combinations of these [13]. However, these may have disadvantages, i.e., high operational costs, toxic reaction by-product production, or, the application may be overly complex, thus reducing likely uptake/use [14].

Adsorption has certain advantages, and can be highly efficient as a method to remove many organic and inorganic pollutants. Further, no reaction by-products are generated with this process, and, it is normally a very simple method (i.e., readily applicable in very low cost/low maintenance systems). A common disadvantage can be the high cost of commercially available sorbent material. This problem could be solved by developing new low-cost sorbents, readily producible from various waste materials. Lignocellulosic biomasses are a good choice because of their physico-chemical properties and structure. To date, various raw waste materials have been used to create biochars and activated carbons: i.e., apricot kernels [15], plum kernels [16,17], olive [18], date and palm stones [19].

Classically, activation of such material has been undertaken using conventional heating methods, at temperatures often up to 900-1000°C. One disadvantage of this (beyond the high energy costs involved) is that heat is applied to the surface of the particulate material involved - which does not then facilitate uniform heating of different size and shape particles. Also, this method often requires several hours of heating to achieve the desired effect [20,21]. Recently, microwave activation has been used as an alternative to conventional heating methods. Microwave activation results in materials receiving energy (which is converted to heat) at a molecular level through dipole rotation and ionic conduction [22]. This technique also takes less time, reducing energy consumption, and particles are heated more uniformly [23]. Further, chemical assisted microwave activation (using base impregnation agents, such as KOH), can help attain a more porous structure and add to the number of positively charged sorption surface sites on the biochar. Hence, this technique can be very applicable when negatively charged species are the target sorbate.

To date, there has been no published research regarding the production of biochar from wild plum kernels (lat. *Prunus cerasifera - Ehrh*) using chemical microwave activation. Therefore, we consider the eventual use of this lignocellulosic material as a new precursor for the production of biochar, which may be applicable to the removal of certain pharmaceuticals from polluted water effluents. This low-cost adsorbent (from a common Serbian waste biomass material) would help address a growing demand in the biochar market. The key questions considered here are: Can wild plum kernels be used to produce a sustainable, high quality biochar; and, can this biochar be utilised to remove emerging pollutants (i.e., pharmaceuticals) from aqueous waste streams? The textural properties and surface chemistry of the WpOH were evaluated, before and after

NPX adsorption; and, adsorption mechanisms involved are discussed in detail. Finally, co-adsorption, using a second pharmaceutical (carbamazepine (CBZ)) was also assessed.

2. Material and Methods

2.1 Materials and chemicals

Ammonium hydroxide (NH_4OH), hydrochloric acid (HCl) and potassium hydroxide (KOH) were purchased from Fisher Scientific, US. NPX was purchased from Sigma–Aldrich, Germany (HPLC grade). Water used for all work was Milli-Q grade Type I (EASYpure® II, Thermo Scientific). Stock solutions of NPX were prepared using 50:50 water (Milli-Q) and acetonitrile (HPLC grade, Sigma-Aldrich, Germany) and the required working solutions were obtained from this. Wild plum kernels were collected from Zrenjanin city, Serbia.

2.2. Biochar preparation

The chemical microwave activation of the wild plum kernels was performed using KOH. The kernels were washed in water and then crushed in a mechanical mill. The milled material was placed in ceramic crucibles and then into an electric furnace, where pyrolysis was carried out. Pyrolysis was achieved in two phases. The first step of pyrolysis involves heating the raw material using the following conditions - rate of 10 °C min^{-1} to 180 °C for 35 minutes. The next step heats the sample up to a higher temperature (rate of 10 °C min^{-1} to 500°C for 60 min). After pyrolysis, the raw biochar was crushed to <2 mm and then soaked in a KOH aqueous solution (50 % w/v). The impregnation ratio was 0.4 g KOH/g biochar. After 24 hours, soaked material was dried in an oven at 110 °C for 2 hours and then placed in ceramic crucibles and introduced

into a microwave where microwave functionalisation was performed for 12 minutes at 700W. The product obtained was rinsed several times with an acidic solution (0.1 mol/L HCl) and then distilled water until the filtrate pH was 7. At the end, the prepared sorbent was dried in an oven at 110 °C for at least 3 h. The final biochar is referred to here as WpOH.

2.3. Characterization of pristine material and WpOH

Bulk elemental analysis was conducted using a Vario EL III C, H, N, S/O Elemental Analyzer (Elementar, Germany). Moisture content, total ash content, suspension pH of the biochar in water (pH_{sus}) and iodide number were determined using American Standard Test Method (ASTM) D2867 - 04, ASTM D2866 - 94, ASTM D6851 - 02 and ASTM D4607 - 14, respectively. The pH_{pzc} (point of zero charge) was also determined (which indicates the net surface charge of the WpOH).

The WpOH yield (an indication of the activation process mass efficiency) was estimated with the equation below:

$$Yield(\%) = \frac{w_b}{w_0} \cdot 100 \quad (1)$$

Where w_0 and w_b (g) are simply the weights of waste biomass and WpOH, respectively. The apparent microstructure of the WpOH was observed using an SEM JSM 6460LV instrument (JEOL, USA), with a dispersive X-ray spectrometer (EDX). Textural properties WpOH were examined by N_2 adsorption-desorption experiment, applying the Brunauer–Emmett–Teller (BET) method on instrument Autosorb iQ (Quantachrome, USA). Surface functionalities were investigated with FTIR spectroscopy on Nexus 670 spectrophotometer (Thermo Nicolet, USA), at wave numbers from 400 to 4000 cm^{-1}. X-

ray diffraction (XRD) tests were carried out to confirm the crystal structure of the biochar using a Rigaku MiniFlex 600 instrument.

2.4. Adsorption experiments

The removal of NPX on synthesized WpOH was studied in batch experiments. During the experiments, a specified mass of WpOH was mixed with 50 mL of solution in a conical flask. Flasks were shaked on a mechanical stirrer (Heidolph Unimax 1010; Heidolph, Germany) at 140 rpm and 22 ± 1 °C. The effects of initial pH (2 - 11), WpOH dosage (2 - 200 mg), contact time (5 - 420 min), initial NPX concentration (3.1 - 125.3 mg/L) and competitive effects with CBZ (10 mg/L) on percentage removal of NPX were studied. pH was adjusted using 0.1 mol/L HCl or 0.1 mol/L NH_4OH and measured using a pH meter (WTW SenTix® 41; WTW, Germany). Suspensions were filtered through Fioroni qualitative filter paper (Grade 115). The removal efficiency, R (%), and the adsorption capacity of NPX, q_e (mg/g), were calculated using equations:

$$R(\%) = \frac{C_0 - C_e}{C_0} \cdot 100 \quad (2)$$

$$q_e = \frac{(C_0 - C_e)}{m} \cdot V \quad (3)$$

Where C_0 is the initial NPX concentration and C_e is the residual NPX concentration (mg/L), V is the volume of solution (L) and m is the mass of the biochar (g). Additionally, isotherm and kinetic parameters were calculated and analysed for errors. In order to understand the NPX adsorption process, the time and concentration dependant data were fitted with kinetic models - a pseudo-first order (PFO), pseudo-second order (PSO) and Weber-Morris intraparticle diffusion model. Moreover, three common isotherm models, Langmuir, Freundlich and Dubinin-Radushkevich (D-R)

were also applied. The theory behind each equation is given within the Supplementary Information (SI).

2.5. Pharmaceutical analysis

Naproxen concentrations in filtered solutions following sorption experiments were quantified by High Performance Liquid Chromatography (HPLC, Agilent 1200 series) coupled to a diode-array detector (DAD). Compound separation was achieved using a C18 column (Zorbax Eclipse XDB-C18, 4.6 mm × 150 mm, particle size 5 μm). The mobile phases used were 0.05% CH_3COOH (in water) and 100% acetonitrile at a 55:45 ratio (isocratic elution). The other parameters used were; flow rate of 1 mL/min; column temperature, 30 °C; injection volume, 15 μL; run time, 18 mins; detection wavelengths monitored were 280, 220, 230 and 254 nm. To allow correction for instrumental drift/sensitivity fluctuations, an external standard was injected between each series of 10 samples.

3. Results and discussion

3.1. Characteristics of the WpOH

3.1.1. Elemental analysis, yield, moisture and ash content

Table S2 summarizes the physico-chemical properties of the pristine wild plum stones and the WpOH. The elemental composition of the kernels is altered during the microwave assisted KOH activation process. The relative elemental content (%) of C dramatically increases (from 52.44 to 88.40 %), while O and H content decreases from 36.98 % to 10.15 % and from 7.63 % to 0.87 % (respectively), due to loss of non-carbon elements and condensation of O-H at high temperatures [24]. Nitrogen also decreases from 2.58 % to 0.58 %. Additionally, all S is lost/volatilised. In terms of yield, a 23 % WpOH yield was achieved. Foo and Hameed (2012a) reported similar

yields for activated carbons prepared by microwave assisted KOH activation from rice husks. This WpOH also had a relatively low moisture and ash content, indicating the high quality of the synthetised biochar [26].

3.1.2. Morphological and textural characteristics

SEM images (with an EDX spectrum) for the WpOH are shown in Fig. 1a-d. It can be seen that the microwave assisted KOH activated WpOH possessed a well-developed porous surface. The roughness and porosity of the WpOH facilitated the capture of NPX molecules within pores and upon surface deformations. The enhanced development of porosity due KOH microwave activation can be represented with the following reaction [27]:

$$6KOH + 2C \rightarrow 2K + 3H_2 + 2K_2CO_3 \quad (4)$$

The diffusion of metallic potassium into the internal structures of the lignocellulosic material will have caused pore spreading and promoted the creation of new pores [25]. During the activation process high temperatures help to improve pore development by promoting the formation and diffusion of metallic potassium molecules into the pores [28]. Using XRD, Raymundo-Pinero et al. [29] determined that K_2CO_3 is formed from KOH at around 400 °C and KOH is consumed at about 600 °C. During microwave activation (>600 °C), and in the presence of a carbonous structure, formed K_2CO_3 may decompose into metallic potassium which is extremely unstable and can react explosively, expanding carbon lattices and creating pores. Consequently, micropore formation can occur more efficiently [30].

N_2 adsorption/desorption isotherms at -196 ºC for WpOH (before/after NPX adsorption) are shown in Fig. 2a. Taking into to account IUPAC classification, a Type I isotherm was evident for the WpOH, which suggests that the WpOH predominantly contains

micropores [31]. Results (Fig. 2a) also showed that the WpOH had a specific surface area of 601.9 m^2/g, a total pore volume of 0.26 cm^3/g, and a micropore and mesopore volume of 0.23 cm^3/g and 0.01 cm^3/g, respectively. These results indicate that wild plum kernel is a good precursor for the production of a high micropore volume biochar (a micropore being defined by IUPAC as a pore smaller than 20 Å in diameter).

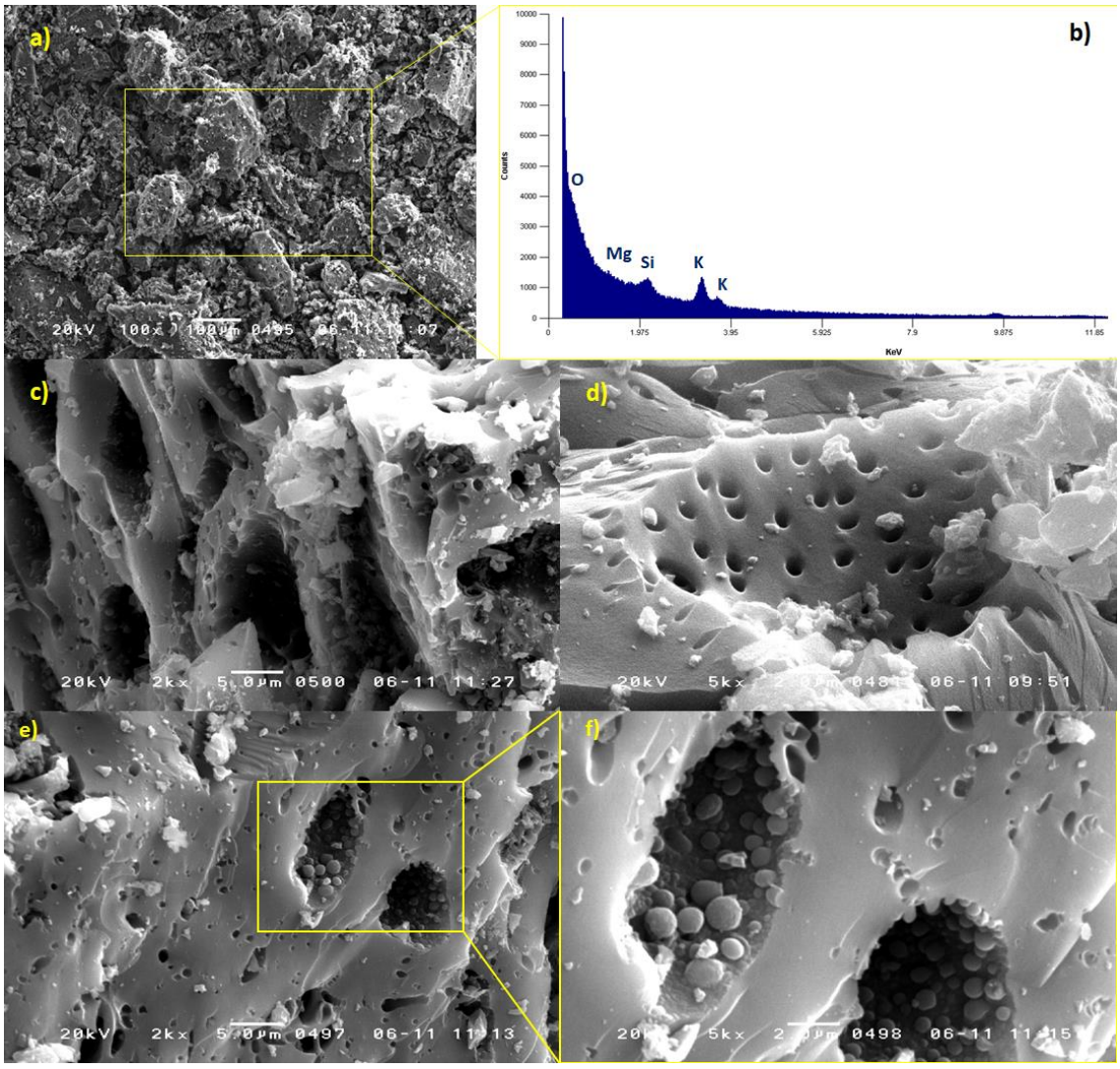

Fig. 1. SEM/EDX micrographs for WpOH at different magnifications before (a-d) and after (e-f) adsorption

3.1.3. XRD analysis

The XRD pattern for the produced WpOH (Fig. 2b) before and after adsorption did not differ significantly. Fig. 2b suggests the WpOH had an amorphous nature with a wide peak in the range of 20 – 30° (2θ = 22.5°) which could be attributed to reflection from (002) graphite planes. The wide hump in the range of 40 – 50° corresponded to (100/101) graphite planes. These peaks are characteristic of amorphous carbonous adsorbents with carbon rings stacked up in a disorderly manner [32]. Due to the presence of numerous micropores, increased background signal between 10 and 20° was detected. These micropores scatter the X-ray beam, causing elevated background signal [33]. This data is in good agreement with the N_2 adsorption isotherm data, which showed a predominance of micropores. The XRD pattern after NPX adsorption showed slightly weaker and wider peaks - suggesting physical surface adsorption on the WpOH surface. Also, there was no change in peak position which further confirms the physical nature of the process [34].

3.1.4. pH_{pzc} and surface functionality

The surface charge of the WpOH was evaluated by pH_{pzc} analysis, where the pH_{pzc} for the WpOH was 7.20 (Table 1 and Fig. 2c), indicative of a near neutral, slightly basic character. The acidic functionality of the WpOH surface is linked with oxygen-containing groups (e.g., carboxylic, anhydrides, lactones and phenols), while the surface basicity is related to the presence of oxygen-free Lewis-type sites and carbonyls, pyrone and chromene type structures [27]. Oxygen-containing functional groups are one of the most common groups formed on the surface of biochars during conventional heating. Microwave activation eliminates some of the acidic oxygen-containing functional groups and makes the WpOH surface more basic. A further shift of the WpOH's pH_{pzc}

towards the basic region (> pH 7) was also likely due to the decomposition of volatile matter during the microwave activation process [35,36].

The WpOH surface chemistry was also studied by FTIR (Fig. 3). Here, a broad peak (in region 3800–3200 cm^{-1}) with maximum at 3741.23 cm^{-1} and minimum at 3443.05 cm^{-1} can be assigned to O-H stretching of hydroxyl groups. Hydroxyl groups can increase the electron donor character of the WpOH. Other small peaks, at 2921.11 and 2853.50 cm^{-1} corresponded to asymmetric and symmetric stretching vibrations of CH, CH_2 and CH_3 groups in carboxylic acid. These functionalities are expected to be strong π-electron acceptors [37]. The band at 1624.84 cm^{-1} may relate to C=C stretching vibrations of olefinic groups [3], while the band at 1067.01 cm^{-1} could be ascribed to C-OH bending vibration [38]. Finally, new peaks at 566.66 and 498.63 cm^{-1} (on saturated WpOH samples) indicate mono-substitute aromatic structures [39]. This is direct evidence of π-π EDA interactions on the WpOH aromatic rings.

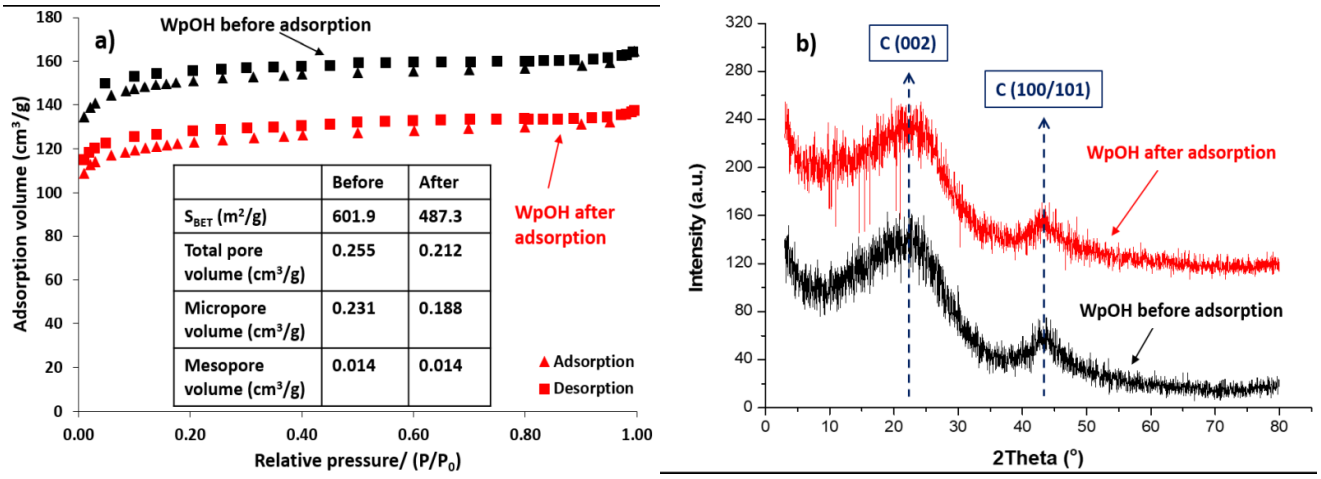

	Before	After
S_{BET} (m^2/g)	601.9	487.3
Total pore volume (cm^3/g)	0.255	0.212
Micropore volume (cm^3/g)	0.231	0.188
Mesopore volume (cm^3/g)	0.014	0.014

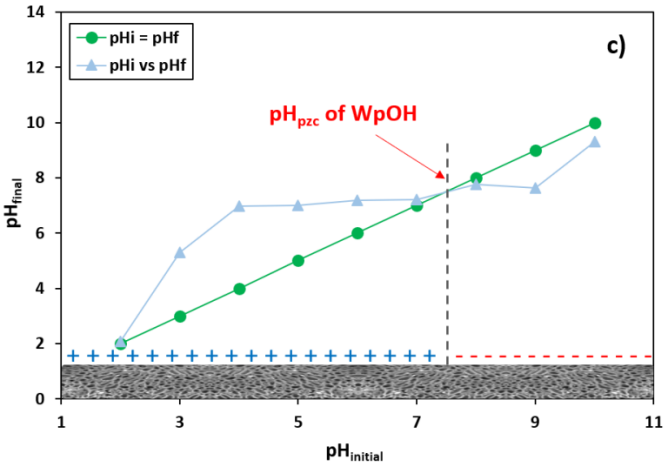

Fig. 2. N_2 adsorption–desorption isotherms (a); XRD patterns before and after adsorption; and (b), pH_{pzc} of WpOH (c)

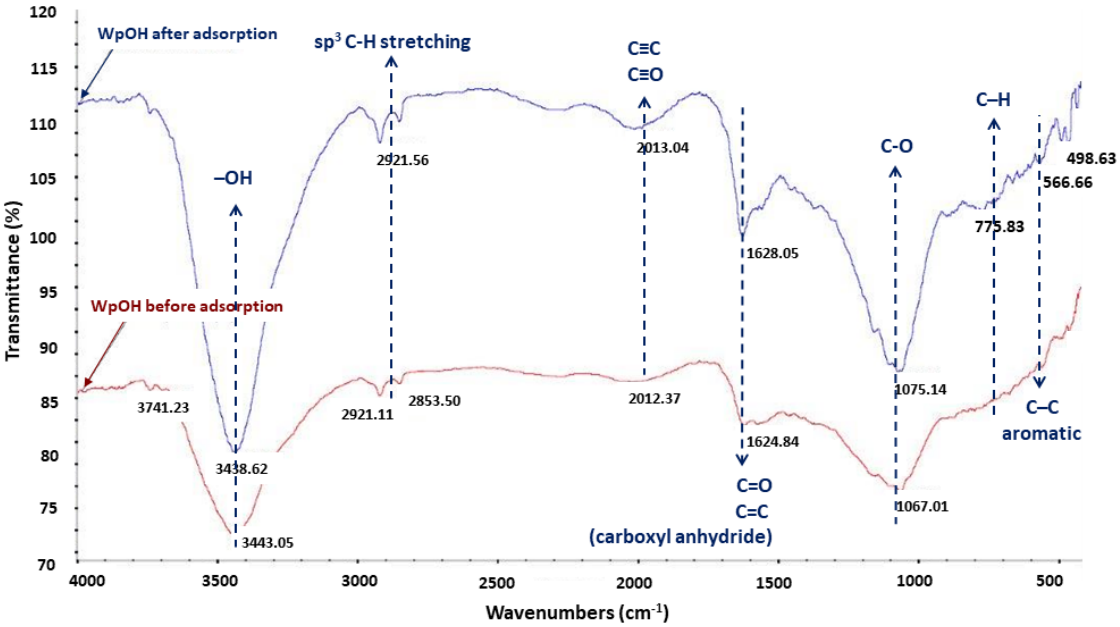

Fig. 3. FTIR spectras of WpOH before and after NPX adsorption

3.2. Single system adsorption studies

3.2.1. pH influence on adsorption

The surface charge (pH_{pzc}) of the WpOH and degree of ionization of NPX is driven by pH. The influence of pH on sorption was demonstrated as a function of adsorption capacity (in mg/g) with respect to solution pH (Fig. 4a). The highest adsorption capacity (≈25 mg/g) was achieved at pH 5 - 7. NPX is an acidic pharmaceutical - with a pKa of 4.2; hence, at pH values > pKa, it is largely in its ionic form (anion) in solution (due to deprotonation). NPX consists of hydrophilic and hydrophobic features. Acidic and hydrophilic activity may occur due to the hydrogen within the carboxylic group, which is ionisable (to its anionic form) at pH's > pKa; while hydrophobic properties are due to the aliphatic rings [40]. In this case, NPX principally exists as a neutral molecule at pH ≤ 4.2, and as NPX^- at pH's > 4.2. Hence, adsorption is very limited at pH's > 7 (since WpOH pH_{pzc} = 7.2) because of the comparatively weaker interactions between the NPX^- anions and the WpOH's negatively charged surface (essentially electrostatic repulsion). A positively charged WpOH surface can be obtained at pH's below the pH_{pzc}, while a negatively charged WpOH surface can be obtained at pH levels above the pH_{pzc}, (preferable for positively charged compound removal). These results are in good agreement with that of Reynel-Avila et al. (2015), who considered NPX removal using bone char – wherein the maximum adsorption capacity was also obtained at pH 7.

3.2.2. Contact time influence and reaction kinetic models

The data regarding contact time and adsorption are presented in Fig. 4b (WpOH dose 0.4 g/L, pH 6). This shows that uptake of NPX was spontaneous and rapid within the first 5-10 minutes, but after this, adsorption slows and equilibrium is reached after ~300 mins for all three initial concentrations. Results also suggest that the adsorption capacity q_t (in mg/g) increases with higher initial concentration. This may be attributed to a higher collision chance between NPX and WpOH surface, higher concentration gradient

and decreased mass transfer resistance. The extended time required to establish equilibrium may indicate that the adsorption process is governed by diffusion and physical adsorption [42,43].

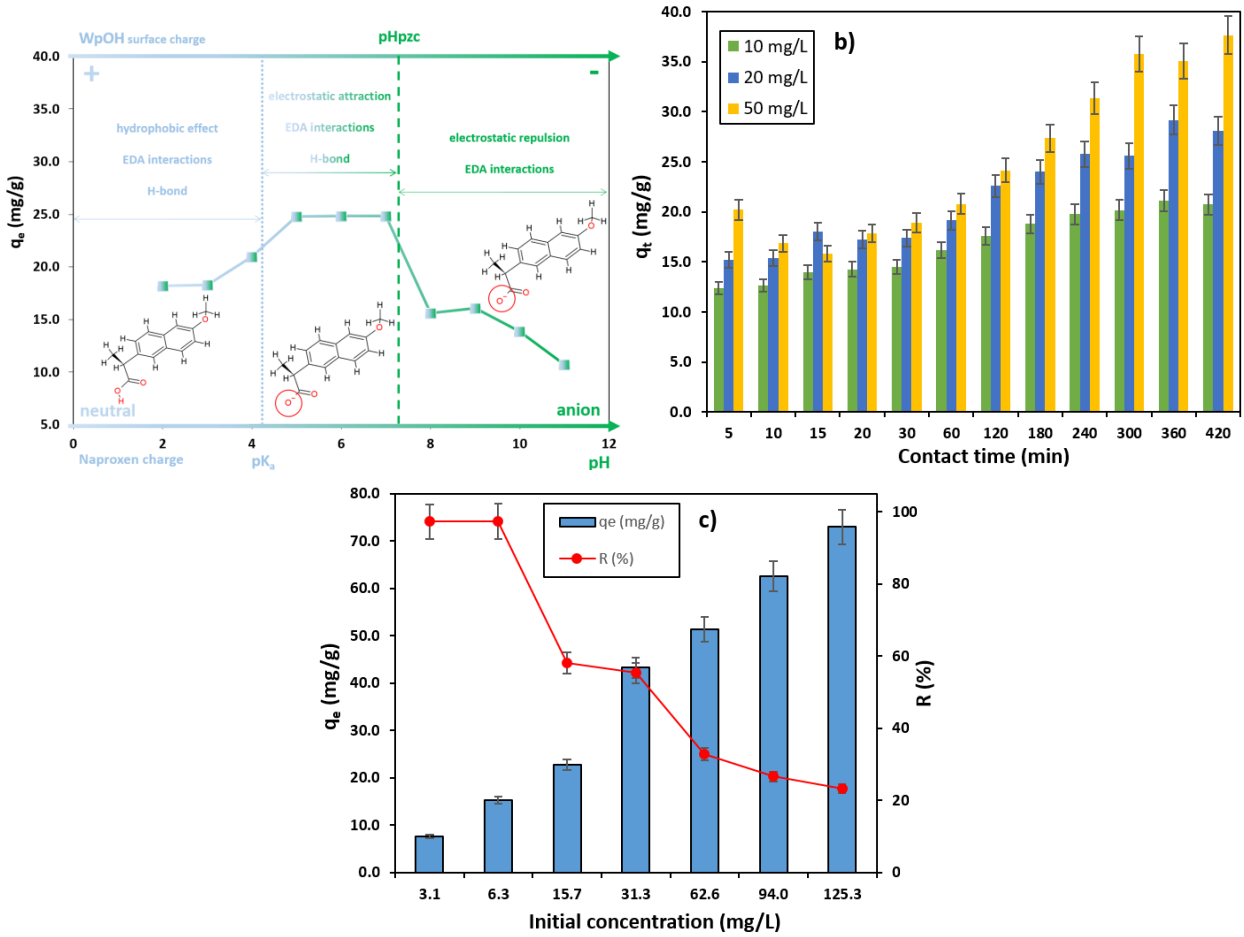

Fig. 4. Influence of pH (a), contact time (b) and initial adsorbate concentration (c) on NPX adsorption

The kinetic model data obtained from the non-linear plots (Fig 5a) are shown in Table 1. Experimental results were consistent with both model, namely pseudo-first order (PFO) and pseudo-second order (PSO) kinetic models (R^2 > 0.92). However, considering the χ^2 and *RMSE* parameters, the PSO values were lower (better) than for the PFO. In addition, $q_{t,\,exp}$ and $q_{t,cal}$ values determined from the PSO model were close.

The suitability of the PSO indicated that chemical interactions between the WpOH and NPX (electrostatic and EDA interactions) have a greater contribution in the adsorption process than pore filling [44]. Similar findings have also been reported previously regarding pharmaceutical removal with activated carbon [45].

Table 1

Kinetic model data for NPX sorption onto WpOH

Pharmaceutical		NPX		
Initial concentration (mg/L)		10	20	50
$q_{t,exp}$ (mg/g)		21.11	29.16	37.65
Pseudo-first-order	$q_{t,cal}$ (mg/g)	8.23	13.03	24.69
	k_1 (min^{-1})	0.01	0.01	0.01
	R^2	0.99	0.96	0.92
	χ^2	4.24	0.95	1.54
	RMSE	2.98	0.51	0.62
Pseudo-second-order	$q_{t,cal}$ (mg/g)	21.33	28.98	38.77
	k_2 (g/mg min)	0.003	0.002	0.001
	R^2	0.99	0.99	0.98
	χ^2	0.01	0.03	0.17
	RMSE	0.03	0.05	0.12
Intraparticle diffusion model	k_i (mg/g $min^{1/2}$)	0.47	0.74	1.26
	C_i (mg/g)	12.08	13.91	11.66
	R^2	0.97	0.96	0.8
	χ^2	0.19	0.33	0.66
	RMSE	0.55	0.84	1.20

3.2.3. Initial adsorbate concentration influence and isotherm models

Adsorption of NPX onto WpOH was investigated at various initial concentrations, from 3.1-125.3 mg/L (at pH 6, WpOH dose 0.4 g/L, reaction temperature 22 ± 1 °C and contact time 180 min). Experimental results are shown in Fig. 4c. It is evident that adsorption was highly dependent on initial NPX concentration. The percentage of NPX adsorption (line on Fig 4c) drops away with increasing initial NPX concentration from 3.1 to 125.3 mg/L. This is due to the limited availability of active adsorption sites on the WpOH surface (given the fixed finite 0.4 g/L dose).

Table 2

Langmuir, Freundlich and Dubinin–Radushkevich isotherm constants for NPX sorption onto WpOH

Langmuir					
$q_{max,exp}$ (mg/g)	q_{max} (mg/g)	K_L (L/mg)	R^2	χ^2	*RMSE*
73.02	73.14	0.13	0.96	0.26	0.11
Freundlich					
K_F ((mg/g)/(mg/L)^n)		$1/n$	R^2	χ^2	*RMSE*
18.39		0.28	0.94	0.04	0.10
Dubinin–Radushkevich					
q_{DR} (mg/g)	K_{DR} (mol^2/J^2)	E_{DR} (kJ/mol)	R^2	χ^2	*RMSE*
47.00	4.81 10^{-8}	3.23	0.81	0.21	0.40

Adsorption isotherms are important tools to help highlight the specific relationship between NPX molecules and the WpOH at the equilibrium stage. Graphical

representations of fitted non-linear isotherm data are shown in Fig. 5b. Additionally, isotherm constant data are presented in Table 2. The isotherms were L-type according to the Giles classification and corresponded to a favourable adsorption process [46]. The best-fit adsorption equilibrium models followed the order: Langmuir > Freundlich > Dubinin-Radushkevich. Isotherm modelling suggested monolayer adsorption of NPX molecules as the Langmuir model describes a homogeneous adsorbent surface with identical adsorption sites. Still, the lowest error values (χ^2 and *RMSE*) were determined for the Freundlich model which assumes heterogeneous adsorptive energy on the adsorbent surface. The maximum monolayer adsorption capacity and the Langmuir constant were estimated as 73.14 mg/g and 0.18 L/mg (respectively). The Freundlich model for NPX adsorption gave a high K_F coefficient (18.39 (mg/g)/(mg/L)^n) which is related to the affinity of the NPX to the adsorbent. Fig 5c clearly shows the failure of the Dubinin–Radushkevich (D-R) isotherm to fit the experimental data. Regardless, E_{DR} can provide some information regarding the adsorption nature. If the E_{DR} is between 8 and 16 kJ/mol, the adsorption process is likely proceeding via chemisorption, while values of E < 8 kJ/mol indicate that the adsorption process is physical in nature [47]. The magnitude of E_{DR} here is 3.226 kJ/mol, indicating that adsorption is mainly via physisorption. However, the poor match of the experimental results with this model points to the limitation of the D-R model in this case.

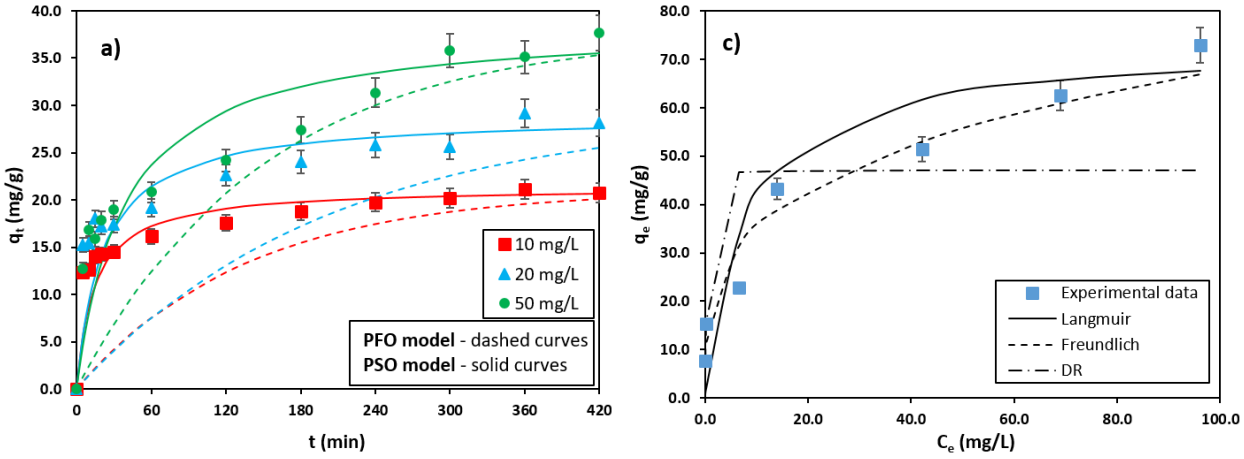

Fig. 5. Adsorption reaction kinetics (a) and isotherms (b) for NPX onto WpOH

In order to compare WpOH with other reported carbonous materials, the maximum adsorption capacity for NPX here was tabulated against that of other similar studies (Table 3). It should be emphasised that a direct comparison between adsorption capacities is very challenging and only indicative because of the different experimental conditions used. For instance, high PhC initial concentrations can also result in large differences in apparent adsorption capacities. For example, in a study by Sarici-Özdemir and Önal [48], the maximum uptake of NPX onto activated carbon from polymeric waste was 400.67 mg/g when the initial NPX concentration was 1000 mg/L, which is highly unrepresentative of any "normal" water environment.

Table 3

Comparison of adsorption capacity (q_{max}) of NPX with other carbonous adsorbents

Adsorbents	q_{max}	Operational conditions						Reference
	(mg/g)	pH	Adsorbent dose (g/L)	Contact time (h)	Concentration (mg/L)	RPM	Temperature (ºC)	
Bone char	4.28	5~7	250	24	50	n.a.	20	[40]
Activated carbon	12.24	7	2	2	50	n.a	25	[48]

biocomposite								
Mesoporous carbon-tubules	17.71	n.a.	35	5	50	150	30 ± 1 ºC	[49]
Silica and magnetic nanoparticle	31.25	n.a.	100 (mg)	4	200	n.a.	n.a.	[50]
Carbon-based magnetic adsorbent	37.58	5	0.3	4	30	120	45	[51]
WpOH	73.14	6	0.4	3	125.3	150	22 ± 1	Present study
Commercial AC	81.00	4	0.1	12	10	n.a.	25 ºC	[52]
Activated carbon from waste apricot	106.38	5.82	2	1	500	400	25	[53]
Activated O-biochar	228	7	2	n.a.	20 (μM)	500	n.a.	[54]

3.3. Mechanism analysis for NPX sorption

Various reaction and mass transfer mechanisms such as electrostatic (coulombic) interactions, H-bonding, π–π and n–π EDA interactions, hydrophobic sorption (London van der Waals forces), intraparticle diffusion and pore filling with pore blocking have been proposed to explain liquid-phase adsorption of organic pollutants from water onto different functionalized biochars [37,49]. Below, we consider the likely mechanisms involved in this study.

3.3.1. Mass transfer mechanism and pore filling

Plots of q_t versus $t^{1/2}$ (Weber-Morris intraparticle diffusion model) are shown in Fig. 6. These plots, for different initial concentrations, are linear and have a relatively high R^2 (0.961–0.976). Intraparticle diffusion is the only rate determining step if the plot of q_t

versus $t^{1/2}$ is linear and passes through the origin ($C_i = 0$). From Table 1, a high R^2 value and low χ^2 and *RMSE* obtained for all concentrations indicated that an intraparticle diffusion mechanism was involved in the adsorption process. However, the plot did not pass through the origin, which indicates that a boundary layer effect may be involved (i.e., intraparticle diffusion was not the only rate-determining step in the overall adsorption process). The nature of the plots indicates that two stages could be involved in NPX removal: surface adsorption, and then, adsorption onto the interior surface of the pores. Namely, adsorption of NPX started with surface interactions with functional groups, until these functionalities were saturated; thereafter, NPX diffused into the WpOH porous structure, adsorbing onto inner pore surfaces [44]. The diffusion rate parameters (K_i) are given in Table 1. The diffusion rate constants, K_i, increased from 0.469 to 1.264 mg/g $min^{1/2}$ (for initial concentrations from 10 to 50 mg/L); while C values decreased which indicates that diffusion was faster at higher concentrations. For porous carbonous materials in general, as pore filling takes place, "pore blocking" will also inevitably occur. Here, the decrease in specific surface area and total pore volume (of WpOH after NPX adsorption) indicated that pore filling certainly contributed to the NPX adsorption mechanism. However, reduced micropore volume was also observed – which suggests that adsorption of NPX resulted in some micropore blocking – as the large molecular size of NPX does not favour adsorption into the micropores of the WpOH. Thus, pore filling was unlikely to be the governing adsorption mechanism here, due to the dominant microporous nature (90% of total pore volume) of the WpOH. Tran et al. [50] came to similar conclusions when studying adsorption of methylene green onto commercial activated charcoal.

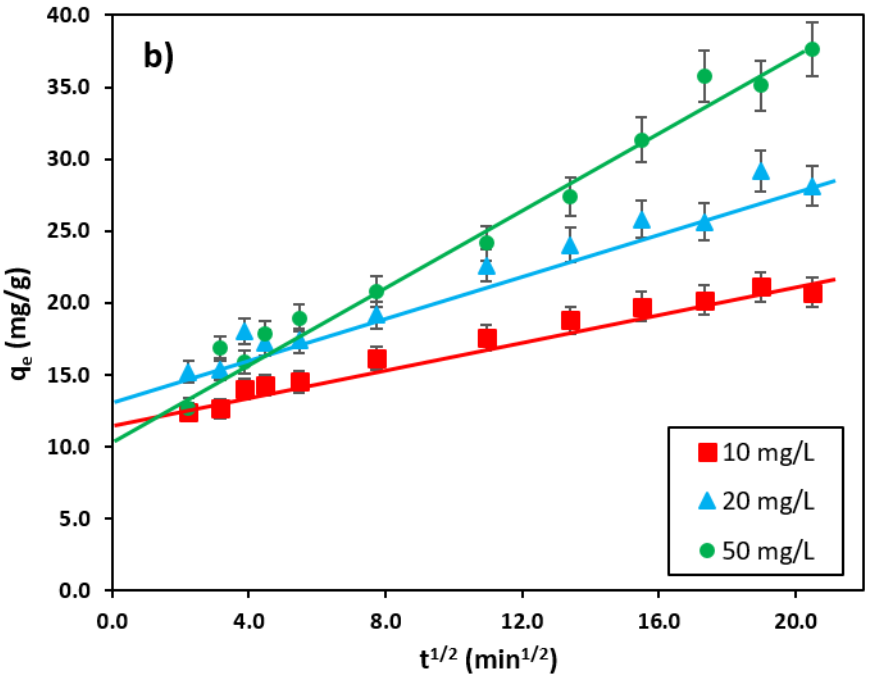

Fig. 6. Weber–Morris intraparticle diffusion plot for NPX onto WpOH

3.3.2. Reaction based adsorption mechanisms

Electrostatic interactions have been discussed as a critical adsorption reaction mechanism in the NPX removal (Sections 3.2.1) hence this interaction is not discussed further.

There are two ways in which the WpOH can interact with the NPX via H-bonding: i.e., as an H-donor or H-acceptor. First, interactions may occur between the hydroxyl groups (H-donors) on the WpOH surface and H-acceptors (oxygen) on the deprotonated NPX molecules. Second, hydroxyl groups on the WpOH may interact with the aromatic rings of the NPX. On the FTIR spectra (Fig. 3), after adsorption, the peak at 3443.05 cm^{-1} corresponded to O-H stretching of hydroxyl groups, and this became more intense and shifted (to 3438.62 cm^{-1}), which confirmed the presence of H-bonding interactions (between the OH group (H-donor) on the WpOH surface and the deprotonated oxygen

on the NPX (H-acceptor)). Additionally, changes in the FTIR spectrum in this wider region (from 3700 cm^{-1} to 3400 cm^{-1}) suggest another type of H-bonding between the –COOH and –OH groups of the WpOH and the aromatic rings of the NPX. Similar results were reported by Song et al. (2017) regarding FTIR spectra for activated carbon, before and after adsorption of NPX.

Biochars with delocalized electrons on their surface possess electron–donor properties. Therefore, electron-donor–acceptor (EDA) interactions likely participated in the adsorption of NPX onto WpOH. π–π EDA interactions occur between π-electrons on a WpOH and π-electrons in the aromatic ring of an adsorbate [52]. Here, graphene C=C bond peaks showed a significant increase in intensity (and shift in peak position from 1624.84 to 1628.05 cm^{-1}) following NPX sorption – which may indicate π–π EDA interactions between the NPX benzene rings and WpOH graphene planes (Fig. 3). Also, peak shifting of carboxylate groups (strong π-electron donors) on the WpOH surface indicated further π-π EDA interactions (with the aromatic rings of the NPX - as π-electron acceptors (Fig. 3). Further, n-π EDA interactions take place when n-electron donors such as oxygen electron pairs of hydroxyl groups interact with electron-depleted sites (π-electron acceptors) on the WpOH. FTIR analysis (Fig. 3) showed a significant increase in the intensity of the C=O and C-O group peaks (1067.01 and 775.83 cm^{-1}, respectively), and a shift in their wavenumber - which suggests the occurrence of n-π EDA interactions on the surface of the WpOH.

A summary of the various proposed adsorption mechanisms at play here are shown on Fig. 7.

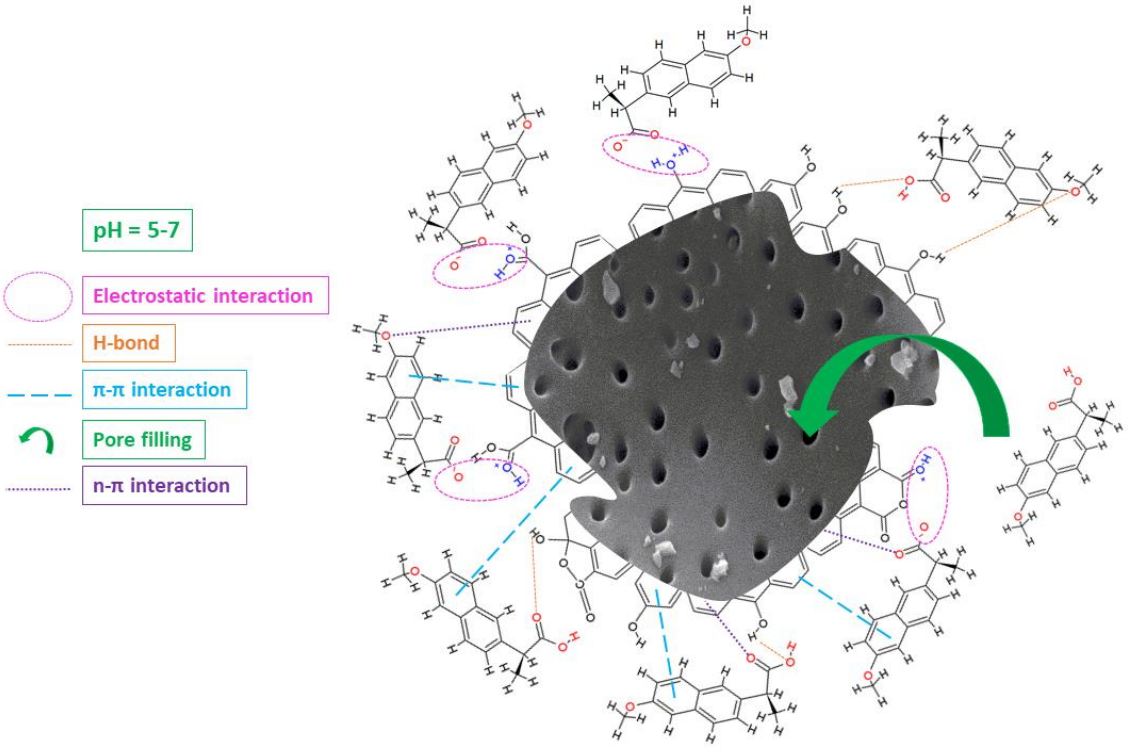

Fig. 7. Proposed key adsorption mechanisms of NPX onto WpOH

3.4. Competitive NPX and CBZ sorption

To begin to compare the effect of individual solute sorption (i.e., of NPX) versus that of sorption of two PhCs onto WpOH, competitive experiments using NPX and CBZ were undertaken (Fig. 8). Here, initial concentrations of NPX and CBZ were 10 mg/L, and the experimental pH was 6.

Surprisingly, no obvious reduction of *R* (%) for NPX was observed when both pharmaceuticals coexisted. Only at lower WpOH doses (2 and 10 mg) do we observe decreased NPX removal as compared to data from the single solute system. This may be because, given the smaller molecular size of CBZ (Table S1), it is easier for CBZ to diffuse into pores when the WpOH concentration in the solution is low. At higher doses of WpOH (80 – 200 mg), almost no competitive adsorption occurred. Since the

structure and characteristics of NPX and CBZ (basic/amphoteric drug) are quite different, the two contaminants seemingly don't compete. The adsorption mechanism in the mixed system may be explained as follows: CBZ (Table S1) under these conditions, exists in its hydrophobic zwitterionic form from pKa 2.3 (ketone group) to pKa 13.9 (amine group - urea). Under the investigated pH (6), zwitterionic CBZ molecules existed in their uncharged form, which suggests there would be little opportunity for electrostatic attraction with the positively charged WpOH [53]. Consequently, the possibility of electrostatic interaction can be almost completely excluded for CBZ, in favour of EDA interactions and H-bonding.

The configuration/structure of NPX and CBZ also exerts a significant effect on interactions with WpOH. Whether a PhC is planar versus nonplanar in structure will affect adsorption [54]. The heterogeneous external surface and the porous nature of the WpOH will tend to provide more favourable adsorption sites for planar molecules than for non-planar molecules, favouring π-π EDA interactions between the conjugated aromatic chromophore skeleton and the biochar. Non-planar molecules are kept away from the adsorbent due to spatial restrictions, resulting in low π-π EDA interactions with the carbonous adsorbent [55,56]. Here, both NPX and CBZ had planar configurations (Fig. S1), however, the more planar structure and smaller molecular size of the CBZ comes to the fore when low WpOH dosing is used, i.e., during the competitive study, which resulted in higher adsorption and faster kinetic characteristics (Fig. 8). Testing adsorption behaviour in mixture scenarios is a very important step when considering applying new adsorbents in large-scale/complex treatment systems.

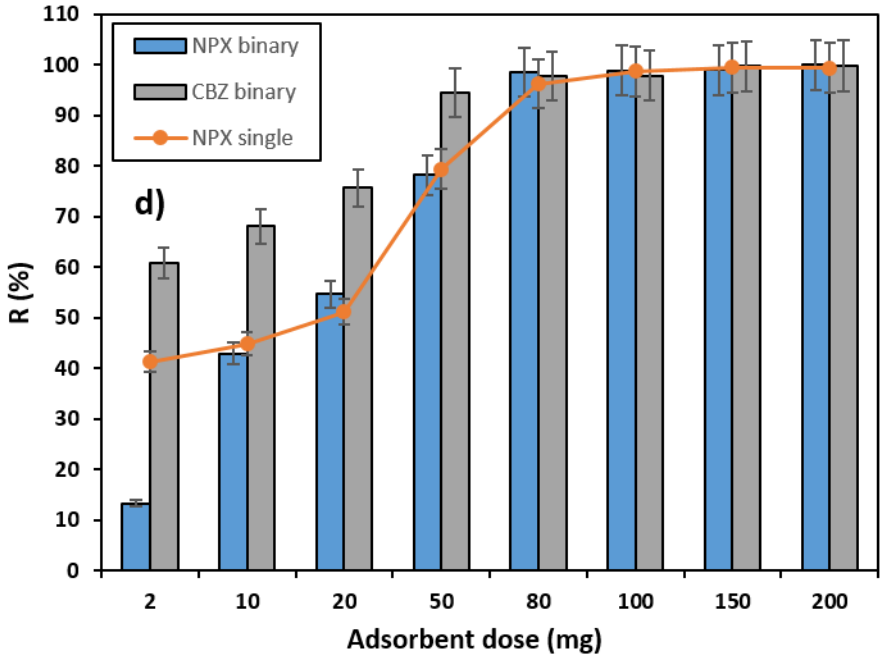

Fig. 8. Competitive adsorption of NPX and CBZ onto WpOH

4. Conclusion

We investigated the adsorption of pharmaceutical compounds (specifically naproxen, and more briefly carbamazepine) onto novel functionalised biochar (WpOH) made from waste plum kernels. Additional WpOH porosity was created by diffusion of metallic potassium into the internal structure of the lignocellulosic material - through a potassium hydroxide assisted microwave activation method. WpOH characterisation showed that the material was dominated by micropores and a variety of surface functionalities (mainly oxygen-containing groups) were present. The removal efficiency of naproxen was strongly dependant on solution pH – with the highest adsorption capacity (73.14 mg/g) occurring at pH 6. Compared to other carbonous adsorbents previously reported [41,57–60] our WpOH had a high adsorption capacity. An adsorption study showed that electrostatic (coulombic) interactions between the WpOH and the naproxen molecules were favoured at optimal pH and within the pH region 5-7

(> the pKa of naproxen but < the pH_{pzc} of WpOH). Additionally, FTIR data indicated that hydrogen bonding, π–π and n–π electron donor-acceptor interactions also contributed to naproxen removal. Due to fundamental differences between naproxen and carbamazepine (i.e., basic vs amphoteric drug), almost no competitive adsorption occurred when both compounds were used as sorbates together. Based on the data presented, it can be concluded that wild plum kernel can act as a sustainable precursor material, and, that potassium hydroxide microwave activation is an efficient preparation method to produce a high quality microporous biochar. This low cost waste material (plum kernel) is abundant in certain countries (i.e., Serbia) and can create a 'green' adsorbent material that has a high adsorption capacity with applicability toward priority pharmaceutical removal from wastewater. In future, this novel activated adsorbent material will be tested against a wider range of pharmaceuticals using real waste water samples – with a view to large scale applicability in scenarios involving pharmaceutical rich waste streams.

Acknowledgments:

The authors acknowledge the financial support by the Ministry of Education, Science and Technological Development of the Republic of Serbia (Projects: III46009 and TR34014). The authors also acknowledge Dr. Kenneth Boyd for his useful advice which helped improve the manuscript.

Appendix A. Supplementary data

E-supplementary data for this work can be found online for this paper.

References

[1] S. Esplugas, D.M. Bila, L.G.T. Krause, M. Dezotti, Ozonation and advanced oxidation technologies to remove endocrine disrupting chemicals (EDCs) and

pharmaceuticals and personal care products (PPCPs) in water effluents, J. Hazard. Mater. 149 (2007) 631–642. doi:10.1016/j.jhazmat.2007.07.073.

[2] B. Silva, F. Costa, I.C. Neves, T. Tavares, Psychiatric Pharmaceuticals as Emerging Contaminants in Wastewater, (2015). doi:10.1007/978-3-319-20493-2.

[3] R.A. Reza, M. Ahmaruzzaman, Removal of naproxen from aqueous environment using porous sugarcane bagasse: Impact of ionic strength, hardness and surfactant, Res. Chem. Intermed. 42 (2016) 1463–1485. doi:10.1007/s11164-015-2097-z.

[4] Á. Sebok, A. Vasanits-Zsigrai, G. Palkó, G. Záray, I. Molnár-Perl, Identification and quantification of ibuprofen, naproxen, ketoprofen and diclofenac present in waste-waters, as their trimethylsilyl derivatives, by gas chromatography mass spectrometry, Talanta. 76 (2008) 642–650. doi:10.1016/j.talanta.2008.04.008.

[5] N. Suriyanon, P. Punyapalakul, C. Ngamcharussrivichai, Mechanistic study of diclofenac and carbamazepine adsorption on functionalized silica-based porous materials, Chem. Eng. J. 214 (2013) 208–218. doi:10.1016/j.cej.2012.10.052.

[6] L. Nielsen, P. Zhang, T.J. Bandosz, Adsorption of carbamazepine on sludge/fish waste derived adsorbents: Effect of surface chemistry and texture, Chem. Eng. J. 267 (2015) 170–181. doi:10.1016/j.cej.2014.12.113.

[7] M.J. Ahmed, B.H. Hameed, Removal of emerging pharmaceutical contaminants by adsorption in a fi xed- bed column : A review, Ecotoxicol. Environ. Saf. 149 (2018) 257–266. doi:10.1016/j.ecoenv.2017.12.012.

[8] P. Villegas-Guzman, J. Silva-Agredo, O. Florez, A.L. Giraldo-Aguirre, C. Pulgarin, R.A. Torres-Palma, Selecting the best AOP for isoxazolyl penicillins

degradation as a function of water characteristics: Effects of pH, chemical nature of additives and pollutant concentration, J. Environ. Manage. 190 (2017) 72–79. doi:10.1016/j.jenvman.2016.12.056.

[9] K.H. Chu, Y.A.J. Al-Hamadani, C.M. Park, G. Lee, M. Jang, A. Jang, N. Her, A. Son, Y. Yoon, Ultrasonic treatment of endocrine disrupting compounds, pharmaceuticals, and personal care products in water: A review, Chem. Eng. J. 327 (2017) 629–647. doi:10.1016/j.cej.2017.06.137.

[10] Y. Wang, H. Huang, X. Wei, Influence of wastewater precoagulation on adsorptive filtration of pharmaceutical and personal care products by carbon nanotube membranes, Chem. Eng. J. 333 (2018) 66–75. doi:10.1016/j.cej.2017.09.149.

[11] N.H. Tran, K.Y.H. Gin, Occurrence and removal of pharmaceuticals, hormones, personal care products, and endocrine disrupters in a full-scale water reclamation plant, Sci. Total Environ. 599–600 (2017) 1503–1516. doi:10.1016/j.scitotenv.2017.05.097.

[12] A. Mirzaei, Z. Chen, F. Haghighat, L. Yerushalmi, Removal of pharmaceuticals and endocrine disrupting compounds from water by zinc oxide-based photocatalytic degradation: A review, Sustain. Cities Soc. 27 (2016) 407–418. doi:10.1016/j.scs.2016.08.004.

[13] S.S.M. Hassan, H.I. Abdel-Shafy, M.S.M. Mansour, Removal of pharmaceutical compounds from urine via chemical coagulation by green synthesized ZnO-nanoparticles followed by microfiltration for safe reuse, Arab. J. Chem. (2016). doi:10.1016/j.arabjc.2016.04.009.

[14] M. Grassi, G. Kaykioglu, V. Belgiorno, Emerging Compounds Removal from Wastewater, (2012) 15–38. doi:10.1007/978-94-007-3916-1.

[15] M. Turk Sekulić, S. Pap, Z. Stojanović, N. Bošković, J. Radonić, T. Šolević Knudsen, Efficient removal of priority, hazardous priority and emerging pollutants with Prunus armeniaca functionalized biochar from aqueous wastes: Experimental optimization and modeling, Sci. Total Environ. 613–614 (2018) 736–750. doi:10.1016/j.scitotenv.2017.09.082.

[16] S. Pap, T. Šolević Knudsen, J. Radonić, S. Maletić, S.M. Igić, M. Turk Sekulić, Utilization of fruit processing industry waste as green activated carbon for the treatment of heavy metals and chlorophenols contaminated water, J. Clean. Prod. 162 (2017) 958–972. doi:10.1016/j.jclepro.2017.06.083.

[17] S. Pap, V. Bezanovic, J. Radonic, A. Babic, S. Saric, D. Adamovic, M. Turk Sekulic, Synthesis of highly-efficient functionalized biochars from fruit industry waste biomass for the removal of chromium and lead, J. Mol. Liq. 268 (2018) 315–325. doi:10.1016/J.MOLLIQ.2018.07.072.

[18] S.M. Yakout, G. Sharaf El-Deen, Characterization of activated carbon prepared by phosphoric acid activation of olive stones, Arab. J. Chem. 9 (2016). doi:10.1016/j.arabjc.2011.12.002.

[19] M.J. Ahmed, Application of agricultural based activated carbons by microwave and conventional activations for basic dye adsorption: Review, J. Environ. Chem. Eng. 4 (2016) 89–99. doi:10.1016/j.jece.2015.10.027.

[20] K.Y. Foo, B.H. Hameed, Microwave-assisted preparation of oil palm fiber activated carbon for methylene blue adsorption, Chem. Eng. J. 166 (2011) 792–

795. doi:10.1016/j.cej.2010.11.019.

[21] M.J. Ahmed, S.K. Theydan, Optimization of microwave preparation conditions for activated carbon from Albizia lebbeck seed pods for methylene blue dye adsorption, J. Anal. Appl. Pyrolysis. 105 (2014) 199–208. doi:10.1016/j.jaap.2013.11.005.

[22] Q.S. Liu, T. Zheng, P. Wang, L. Guo, Preparation and characterization of activated carbon from bamboo by microwave-induced phosphoric acid activation, Ind. Crops Prod. 31 (2010) 233–238. doi:10.1016/j.indcrop.2009.10.011.

[23] D. Xin-hui, C. Srinivasakannan, P. Jin-hui, Z. Li-bo, Z. Zheng-yong, Comparison of activated carbon prepared from Jatropha hull by conventional heating and microwave heating, Biomass and Bioenergy. 35 (2011) 3920–3926. doi:10.1016/j.biombioe.2011.06.010.

[24] H. Jin, S. Capareda, Z. Chang, J. Gao, Y. Xu, J. Zhang, Biochar pyrolytically produced from municipal solid wastes for aqueous As(V) removal: Adsorption property and its improvement with KOH activation, Bioresour. Technol. 169 (2014) 622–629. doi:10.1016/j.biortech.2014.06.103.

[25] K.Y. Foo, B.H. Hameed, Microwave-assisted preparation and adsorption performance of activated carbon from biodiesel industry solid reside: Influence of operational parameters, Bioresour. Technol. 103 (2012) 398–404. doi:10.1016/j.biortech.2011.09.116.

[26] H.N. Tran, S.J. You, H.P. Chao, Effect of pyrolysis temperatures and times on the adsorption of cadmium onto orange peel derived biochar, Waste Manag. Res. 34 (2016) 129–138. doi:10.1177/0734242X15615698.

[27] K.Y. Foo, B.H. Hameed, Coconut husk derived activated carbon via microwave induced activation: Effects of activation agents, preparation parameters and adsorption performance, Chem. Eng. J. 184 (2012) 57–65. doi:10.1016/j.cej.2011.12.084.

[28] I.A.W. Tan, A.L. Ahmad, B.H. Hameed, Adsorption of basic dye using activated carbon prepared from oil palm shell: batch and fixed bed studies, Desalination. 225 (2008) 13–28. doi:10.1016/j.desal.2007.07.005.

[29] E. Raymundo-Piñero, P. Azaïs, T. Cacciaguerra, D. Cazorla-Amorós, A. Linares-Solano, F. Béguin, KOH and NaOH activation mechanisms of multiwalled carbon nanotubes with different structural organisation, Carbon N. Y. 43 (2005) 786–795. doi:10.1016/j.carbon.2004.11.005.

[30] C. Rodriguez Correa, T. Otto, A. Kruse, Influence of the biomass components on the pore formation of activated carbon, Biomass and Bioenergy. 97 (2017) 53–64. doi:10.1016/j.biombioe.2016.12.017.

[31] K.S.W. Sing, Reporting physisorption data for gas/solid systems with special reference to the determination of surface area and porosity (Recommendations 1984), Pure Appl. Chem. 57 (1985) 603–619.

[32] Y. bin Tang, Q. Liu, F. yan Chen, Preparation and characterization of activated carbon from waste ramulus mori, Chem. Eng. J. 203 (2012) 19–24. doi:10.1016/j.cej.2012.07.007.

[33] L. Muniandy, F. Adam, A.R. Mohamed, E.P. Ng, The synthesis and characterization of high purity mixed microporous/mesoporous activated carbon from rice husk using chemical activation with NaOH and KOH, Microporous

Mesoporous Mater. 197 (2014) 316–323. doi:10.1016/j.micromeso.2014.06.020.

[34] S. Banerjee, G.C. Sharma, R.K. Gautam, M.C. Chattopadhyaya, S.N. Upadhyay, Y.C. Sharma, Removal of Malachite Green, a hazardous dye from aqueous solutions using Avena sativa (oat) hull as a potential adsorbent, J. Mol. Liq. 213 (2016) 162–172. doi:10.1016/j.molliq.2015.11.011.

[35] R. Hoseinzadeh Hesas, W.M.A. Wan Daud, J.N. Sahu, A. Arami-Niya, The effects of a microwave heating method on the production of activated carbon from agricultural waste: A review, J. Anal. Appl. Pyrolysis. 100 (2013) 1–11. doi:10.1016/j.jaap.2012.12.019.

[36] Y. Kan, Q. Yue, B. Gao, Q. Li, Comparison of activated carbons from epoxy resin of waste printed circuit boards with KOH activation by conventional and microwave heating methods, J. Taiwan Inst. Chem. Eng. 68 (2016) 440–445. doi:10.1016/j.jtice.2016.08.047.

[37] M. Kah, G. Sigmund, F. Xiao, T. Hofmann, Sorption of ionizable and ionic organic compounds to biochar, activated carbon and other carbonaceous materials, Water Res. 124 (2017) 673–692. doi:10.1016/j.watres.2017.07.070.

[38] V.O. Njoku, K.Y. Foo, M. Asif, B.H. Hameed, Preparation of activated carbons from rambutan (Nephelium lappaceum) peel by microwave-induced KOH activation for acid yellow 17 dye adsorption, Chem. Eng. J. 250 (2014) 198–204. doi:10.1016/j.cej.2014.03.115.

[39] E. Kaçan, C. Kütahyali, Adsorption of strontium from aqueous solution using activated carbon produced from textile sewage sludges, J. Anal. Appl. Pyrolysis. 97 (2012) 149–157. doi:10.1016/j.jaap.2012.06.006.

[40] A.D. Dwivedi, K. Gopal, R. Jain, Strengthening adsorption characteristics of non-steroidal anti-inflammatory drug onto microwave-assisted mesoporous material: Process design, mechanism and characterization, Chem. Eng. J. 168 (2011) 1279–1288. doi:10.1016/J.CEJ.2011.02.041.

[41] H.E. Reynel-Avila, D.I. Mendoza-Castillo, A. Bonilla-Petriciolet, J. Silvestre-Albero, Assessment of naproxen adsorption on bone char in aqueous solutions using batch and fixed-bed processes, J. Mol. Liq. 209 (2015) 187–195. doi:10.1016/j.molliq.2015.05.013.

[42] L. Rafati, M.H. Ehrampoush, A.A. Rafati, M. Mokhtari, A.H. Mahvi, Modeling of adsorption kinetic and equilibrium isotherms of naproxen onto functionalized nano-clay composite adsorbent, J. Mol. Liq. 224 (2016) 832–841. doi:10.1016/j.molliq.2016.10.059.

[43] A.B. Albadarin, C. Mangwandi, A.H. Al-Muhtaseb, G.M. Walker, S.J. Allen, M.N.M. Ahmad, Kinetic and thermodynamics of chromium ions adsorption onto low-cost dolomite adsorbent, Chem. Eng. J. 179 (2012) 193–202. doi:10.1016/j.cej.2011.10.080.

[44] S. Álvarez-Torrellas, M. Muñoz, J.A. Zazo, J.A. Casas, J. García, Synthesis of high surface area carbon adsorbents prepared from pine sawdust-Onopordum acanthium L. for nonsteroidal anti-inflammatory drugs adsorption, J. Environ. Manage. 183 (2016) 294–305. doi:10.1016/j.jenvman.2016.08.077.

[45] V. Calisto, C.I.A. Ferreira, J.A.B.P. Oliveira, M. Otero, V.I. Esteves, Adsorptive removal of pharmaceuticals from water by commercial and waste-based carbons, J. Environ. Manage. 152 (2015) 83–90. doi:10.1016/j.jenvman.2015.01.019.

[46] C.H. Giles, T.H. MacEwan, S.N. Nakhwa, D. Smith, 786. Studies in adsorption. Part XI. A system of classification of solution adsorption isotherms, and its use in diagnosis of adsorption mechanisms and in measurement of specific surface areas of solids, J. Chem. Soc. (1960) 3973–3993.

[47] H.N. Tran, S.J. You, A. Hosseini-Bandegharaei, H.P. Chao, Mistakes and inconsistencies regarding adsorption of contaminants from aqueous solutions: A critical review, Water Res. 120 (2017) 88–116. doi:10.1016/j.watres.2017.04.014.

[48] Ç. Sarici-Özdemir, Y. Önal, Study to observe the applicability of the adsorption isotherms used for the adsorption of medicine organics onto activated carbon, Part. Sci. Technol. 36 (2018) 254–261. doi:10.1080/02726351.2016.1246497.

[49] M.B. Ahmed, J.L. Zhou, H.H. Ngo, W. Guo, M. Chen, Progress in the preparation and application of modified biochar for improved contaminant removal from water and wastewater, Bioresour. Technol. 214 (2016) 836–851. doi:10.1016/j.biortech.2016.05.057.

[50] H.N. Tran, Y.F. Wang, S.J. You, H.P. Chao, Insights into the mechanism of cationic dye adsorption on activated charcoal: The importance of Π–Π interactions, Process Saf. Environ. Prot. 107 (2017) 168–180. doi:10.1016/j.psep.2017.02.010.

[51] J.Y. Song, B.N. Bhadra, S.H. Jhung, Microporous and Mesoporous Materials Contribution of H-bond in adsorptive removal of pharmaceutical and personal care products from water using oxidized activated carbon, Microporous Mesoporous Mater. 243 (2017) 221–228. doi:10.1016/j.micromeso.2017.02.024.

[52] X. Tan, Y. Liu, G. Zeng, X. Wang, X. Hu, Y. Gu, Z. Yang, Application of biochar for the removal of pollutants from aqueous solutions, Chemosphere. 125 (2015) 70–85. doi:10.1016/j.chemosphere.2014.12.058.

[53] M. Turk Sekulic, N. Boskovic, A. Slavkovic, J. Garunovic, S. Kolakovic, S. Pap, Surface functionalised adsorbent for emerging pharmaceutical removal: Adsorption performance and mechanisms, Process Saf. Environ. Prot. 125 (2019) 50–63. doi:10.1016/j.psep.2019.03.007.

[54] S. Wang, X. Li, H. Zhao, X. Quan, S. Chen, H. Yu, Enhanced adsorption of ionizable antibiotics on activated carbon fiber under electrochemical assistance in continuous-flow modes, Water Res. 134 (2018) 162–169. doi:10.1016/j.watres.2018.01.068.

[55] W. Konicki, M. Aleksandrzak, D. Moszyński, E. Mijowska, Adsorption of anionic azo-dyes from aqueous solutions onto graphene oxide: Equilibrium, kinetic and thermodynamic studies, J. Colloid Interface Sci. 496 (2017) 188–200. doi:10.1016/j.jcis.2017.02.031.

[56] G. Ersan, O.G. Apul, F. Perreault, T. Karanfil, Adsorption of organic contaminants by graphene nanosheets: A review, Water Res. 126 (2017) 385–398. doi:10.1016/j.watres.2017.08.010.

[57] D. Saloglu, N. Ozcan, Activated carbon embedded chitosan/polyvinyl alcohol biocomposites for adsorption of nonsteroidal anti-inflammatory drug-naproxen from wastewater, Desalin. Water Treat. 107 (2018) 72–84.

[58] S.P. Dubey, A.D. Dwivedi, C. Lee, Y.N. Kwon, M. Sillanpaa, L.Q. Ma, Raspberry derived mesoporous carbon-tubules and fixed-bed adsorption of

pharmaceutical drugs, J. Ind. Eng. Chem. 20 (2014) 1126–1132. doi:10.1016/j.jiec.2013.06.051.

[59] M. Kazem, M. Nodeh, M. Radfard, L. Ali, H.R. Nodeh, Enhanced removal of naproxen from wastewater using silica magnetic nanoparticles decorated onto graphene oxide ; parametric and equilibrium study, Sep. Sci. Technol. 53 (2018) 2476–2485. doi:10.1080/01496395.2018.1457054.

[60] Z. İlbay, S. Şahin, Kerkez, S. Bayazit, Isolation of naproxen from wastewater using carbon-based magnetic adsorbents, Int. J. Environ. Sci. Technol. 12 (2015) 3541–3550. doi:10.1007/s13762-015-0775-4.

Supplementary materials

Ionisable emerging pharmaceutical adsorption onto microwave functionalised biochar derived from novel lignocellulosic waste biomass

Olivera Paunovic[a], Sabolc Pap[a,b,‡], Snezana Maletic[c], Mark A. Taggart[b], Nikola Boskovic[a], Maja Turk Sekulic[a,§]

[a] *University of Novi Sad, Faculty of Technical Sciences, Department of Environmental Engineering and Occupational Safety and Health, Trg Dositeja Obradovica 6, Novi Sad, Serbia*

[b] *Environmental Research Institute, North Highland College, University of the Highlands and Islands, Thurso, Scotland, KW14 7JD, UK*

[c] *University of Novi Sad, Faculty of Science, Department of Chemistry, Biochemistry and Environmental Protection, Trg Dositeja Obradovića 3, Novi Sad, Serbia*

[‡]Corresponding author at: Environmental Research Institute, North Highland College, University of the Highlands and Islands, Thurso, Scotland, KW14 7JD, UK
[§]Corresponding author at: Department of Environmental Engineering and Occupational Safety and Health, Faculty of Technical Sciences, University of Novi Sad, Trg Dositeja Obradovica 6, Novi Sad, Serbia
E-mail addresses: sabolcpap@uns.ac.rs; szabolcs.pap@uhi.ac.uk (Sabolc Pap); majaturk@uns.ac.rs (Maja Turk Sekulic)

Adsorption models

Pseudo-first order (PFO) kinetic model [1]:

$$\log(q_e - q_t) = \log q_e - \left(\frac{k_1}{2.303}\right)t \quad (S1)$$

Pseudo-second order (PSO) kinetic model [2,3]:

$$\frac{t}{q_t} = \frac{1}{k_2 q_e^2} + \frac{1}{q_e}t \quad (S2)$$

Weber–Morris intraparticle diffusion model [4]:

$$q_t = k_i t^{1/2} + C_i \quad (S3)$$

Langmuir isotherm model [5]:

$$\frac{C_e}{q_e} = \frac{1}{q_{max} K_L} + \frac{C_e}{q_{max}} \quad (S4)$$

Freundlich isotherm model [6]:

$$log q_e = log K_F + n log C_e \quad (S5)$$

Dubinin-Radushkevich (D-R) isotherm model [7]:

$$ln q_e = ln q_{DR} - K_{DR}\varepsilon^2 \quad (S6)$$

Adsorption energy equation:

$$E = \frac{1}{\sqrt{-2K_{DR}}} \quad (S7)$$

Polanyi potential equation:

$$\varepsilon = RT ln\left(1 + \frac{1}{C_e}\right) \quad (S8)$$

Nonlinear chi-square test (χ^2) and the root mean square error (*RMSE*) [8]:

$$\chi^2 = \sum_{i=1}^{N} \frac{(q_e^{exp} - q_e^{cal})^2}{q_e^{cal}} \quad (S9)$$

$$RMSE = \sqrt{\frac{1}{N-2}\sum_{i=1}^{N}(q_e^{exp} - q_e^{cal})^2} \qquad (S10)$$

k_1 (min^{-1}) - PFO rate constant; k_2 (g/mg min) - PSO rate constant; k_i ($mg/g\ min^{1/2}$) - intraparticle diffusion rate constant; C_i (mg/g) - constant proportional to the boundary layer thickness; K_L (L/mg) - Langmuir equilibrium constant; q_{max} and q_{DR} (mg/g) - maximum monolayer saturation capacity; K_F ($(mg/g)/(mg/L)^n$) - Freundlich isotherm constant; n - Freundlich exponent; K_{DR} (mol^2/J^2) - isotherm coefficient; E (kJ/mol) - mean free adsorption energy; ε - Polanyi potential, R (8.314 J/mol K) - universal gas constant, T (K) - absolute temperature; q_e^{exp} - observation from the adsorption experiment, q_e^{cal} - calculated PhC adsorption capacity; N - number of the samples.

Table S1

Structure and properties of the two pharmaceuticals studied here.

Drug/ CAS number/ EC number/ Formula	Molecular structure	Molecular weight (g/mol)	pKa	Solubility in water (mg/L)	Log K_{ow}	Molecular diameter (Å)
Naproxen[1]/ 22204-53-1/ 245-969-2/ $C_{14}H_{14}O_3$	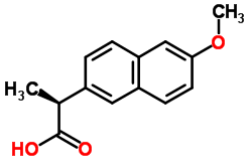	230.263	4.2	1-3	3.18	Min. 7.7 Max 12.6
Carbamazepine[2]/ 298-46-4/ 206-062-7/ $C_{15}H_{12}N_2O$	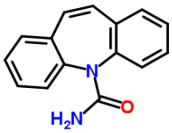	236.274	2.3 and 13.9	17.66	2.25	Min. 6.5 Max. 11.7

[1]NSAID, analgesic and antipyretic;[9,10]

[2]Antiepileptic; [11]

Table S2

Characteristics of the raw material and the biochar

Material		Wild plum stones	WpOH
Elemental analysis	C	52.44	88.40
(%)	O[a]	36.98	10.15
	S	0.37	-
	N	2.58	0.58
	H	7.63	0.87
Ash content (%)		3.4	4
Moisture content (%)		6.1	5.51
pH_{sus}		7	8
Iodide number		-	400
pH_{pzc}		-	7.2
Yield (%)		-	23

[a]By difference

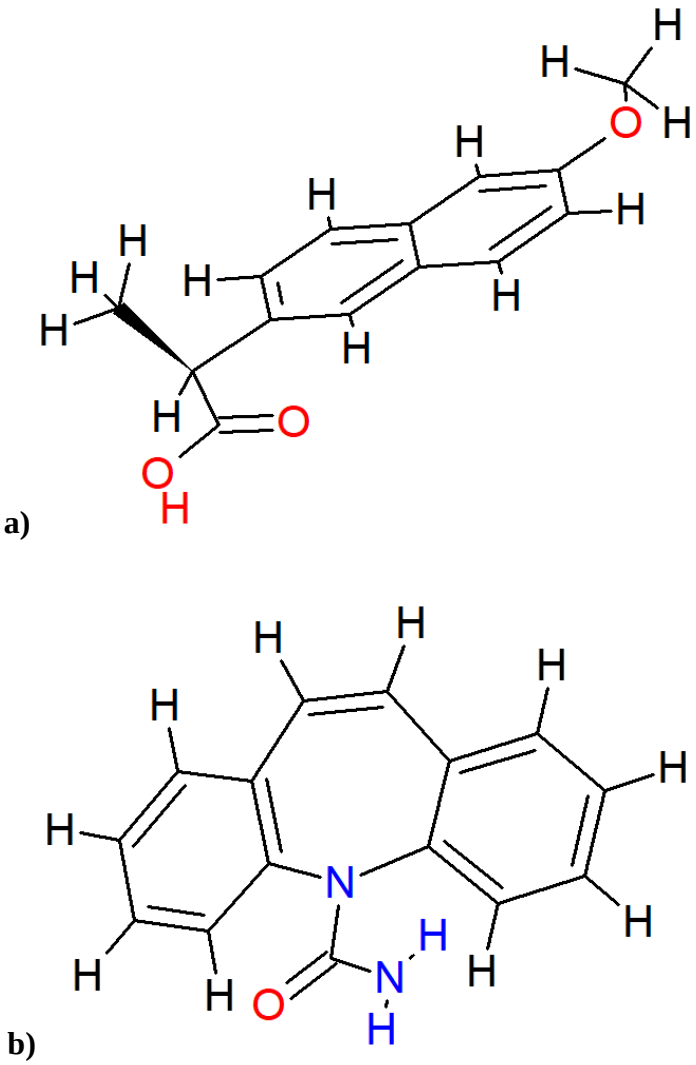

Fig. S1. Configuration of PhC molecules in space: planar naproxen (a) and planar carbamazepine (b)

References

[1] S. Lagergren, About the theory of so-called adsorption of soluble substances, Kongl. Vetenskaps Acad. Handl. 24 (1898) 1–39.

[2] Y.S. Ho, G. McKay, Pseudo-second order model for sorption processes, Process Biochem. 34 (1999) 451–465.

[3] G. Blanchard, M. Maunaye, G. Martin, Removal of heavy metals from waters by means of natural zeolites, Water Res. 18 (1984) 1501–1507.

[4] W.J. Weber, J.C. Morris, Kinetics of adsorption on carbon from solution, J. Sanit. Eng. Div. 89 (1963) 31–60.

[5] I. Langmuir, The Adsorption of Gases on Plane Surfaces of Glass, Mica and Platinum, J. Am. Chem. Soc. 40 (1918) 1361–1403.

[6] H. Freundlich, Über die adsorption in lösungen, Zeitschrift Für Phys. Chemie. 57 (1907) 385–470.

[7] M.M. Dubinin, E.D. Zaverina, L.V. Radushkevich, Sorption and structure of active carbons. I. Adsorption of organic vapors, Zhurnal Fiz. Khimii. 21 (1947) 1351–1362.

[8] K.Y. Foo, B.H. Hameed, Insights into the modeling of adsorption isotherm systems, Chem. Eng. J. 156 (2010) 2–10.

[9] Y. Gao, M.A. Deshusses, Adsorption of clofibric acid and ketoprofen onto powdered activated carbon: Effect of natural organic matter, Environ. Technol. 32 (2011) 1719–1727.

[10] S. Das, Micropollutants in Wastewater: Fate and Removal Processes, in: N.M. Ray (Ed.), Physico-Chemical Wastewater Treat. Resour. Recover., IntechOpen, Rijeka, 2017: p. Ch. 5.

[11] M. To, P. Hadi, C. Hui, C. Sze, K. Lin, G. Mckay, Mechanistic study of atenolol , acebutolol and carbamazepine adsorption on waste biomass derived activated carbon, J. Mol. Liq. 241 (2017) 386–398.